

Simulation of reclaimed ground composed of dredged soil for two kinds of earthquake ground motions with different spectral characteristics

Kai Sun*, Eiji Yamada**, Masaki Nakano*** and Akira Asaoka****

* Member M. of Eng. Doctoral student Dept. of Civil Eng. Nagoya Univ. (Chikusa, Nagoya 464-8603)

**Member Dr. of Eng. Research Engineer, Chubu Electric Power Company, Incorporated
(20-1, Kitasekiyama, Ootaka, Midori, Nagoya, 459-8522)

***Member Dr. of Eng. Prof. Nagoya Univ. (Chikusa, Nagoya 464-8603)

****Member Dr. of Eng. Senior Research Advisor, Association for the Development of Earthquake Prediction
(1-5-8, Sarugaku, Chiyoda, Tokyo, 101-0064)

In this research, the co-seismic and post-seismic behaviors of an offshore artificial island composed of dredged soil under two kinds of earthquake ground motions, which are short-period (Type 1) and long-period (Type 2), are investigated by using a soil-water coupled finite element analysis code—*GEOASIA*. The parameters used in the calculation are obtained by the simulation of a series of mechanical tests using the SYS Cam-clay model. In the analysis, the construction history was considered by way of simulating the construction of embankment and reclamation of ground. Compared with the short-period motion, different results are obtained under the long-period motion: 1) larger deformations during the earthquake, both vertical settlement and horizontal displacement, are caused by long-period motion due to the larger shear strain, 2) in some part of the ground, larger post-seismic settlement caused by long-period motion due to the decay of soil structure, and 3) in the soil element with significant shear strain, volume expansion is observed during earthquake, which is usually regarded as an undrained simple shear process. For clay ground, the settlement after earthquake lasts for long time and the amount of settlement is large.

Key words: numerical analysis, seismic response, reclaimed ground, construction history

1. Introduction

The Port of Nagoya is a shallow-depth artificial harbor that has been constructed through repeated dredging and landfilling. The dredged soil in the Port of Nagoya of about 1.3 million m³ is generated per year. An offshore artificial island that serves as a temporary disposal for dredged soil is located at the entrance of the port. However, the predicted Tokai-Tonankai Earthquake will occur around the Chubu District of Japan in the near future. It is very important to know whether the function of the Port of Nagoya can be maintained after the Earthquake, and to evaluate the co-seismic and post-seismic responses of an artificial island due to the high possibility of major earthquake in Nagoya region.

Recently, elaborate finite element approaches¹⁾⁻⁴⁾ have been used to analyse the seismic behaviors of the reclaimed ground. In the past analysis, the construction of structure, which greatly affects the loading history and the current state distribution of the soil, was seldom considered. Moreover, for the reclaimed ground composed of dredged soil, it is difficult to describe the soil properties by a constitutive model as well as to calculate the behavior of the soil ground during /after the earthquake.

In this study, seismic response analysis on an offshore artificial island mainly composed of dredged soil, is carried out with the aim of extracting the problems that may arise in the case that subduction zone earthquakes occur. Two types of ground motions with different spectral characteristics are then applied on the rigid engineering bedrock respectively. Subsequently, the behaviors of the reclaimed ground during and after the earthquake under plane strain condition are investigated by using the static/dynamic soil-water coupled finite element analysis code *GEOASIA*^{5), 6)}. In the analysis code, the SYS Cam-clay model⁷⁾⁻⁹⁾ is used as a constitutive equation for the soil skeleton. It is available in a wide range, from clay through intermediate soil to sand within a single theory system merely by controlling the rate of loss of overconsolidation, decay of structure and development of induced anisotropy. The validity of performance of *GEOASIA* has been verified through the deformation and failure analysis not only under dynamic loading but also under static loading. More details are in references^{10), 11)}.

In order to obtain the current state distribution of the soils by considering the stress history, the construction process, including the construction of embankment and reclamation of dredged soil, is reproduced according to

the actual construction history by using the analysis code *GEOASIA*^{5), 6)}. A series of laboratory tests results and ground survey data are used to determine the material constants and the initial values (before construction) by using the SYS Cam-clay model⁷⁾⁻⁹⁾.

For the ground mainly consists of naturally deposited clayey soil, attention should be paid to large settlement of clay layer during/after earthquake and large horizontal displacement near the retaining wall. The analysis results of the island, including the pre-seismic (construction and consolidation processes), co-seismic and post-seismic mechanical behaviors, are interpreted in the theory frame of the SYS Cam-clay model based on the concept of soil skeleton structure (structure, overconsolidation and anisotropy).

2. Determination of soil parameters of seabed ground and reclaimed ground

2.1 Soil layers distribution

This research focuses on the mechanical behaviors of the artificial island composed of a reclaimed ground of dredged soil and a seabed ground. The seabed ground mainly consists of naturally deposited clay and silty clay. The distribution of soil layers and the structures on the island are shown in **Fig. 1**. Based on the ground investigation, the initial ground is assumed to be horizontally homogeneous and can be divided into six layers, from bottom to top, which are an alluvial clay layer (AcL layer), an alluvial sand layer (As layer), three alluvial clay layers (AcU3 layer, AcU2 layer and AcU1 layer) and a reclaimed layer of dredged soil (Bc layer), respectively. The thickness of them is 7.5 m, 2.5 m, 10 m, 10 m, 6 m and 20 m, respectively and the total is 56 m.

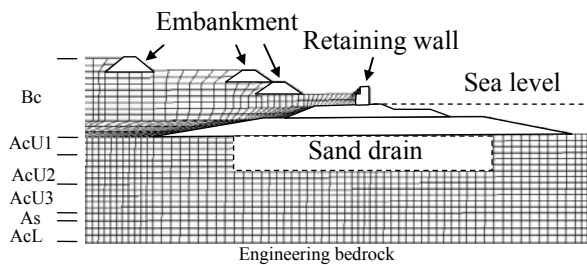


Fig. 1 Distribution of soil layers and structures on the artificial island

As shown in **Fig. 1**, in order to accelerate the consolidation of clay layer, an area in AcU1 layer and AcU2 layer was improved by sand drain, on which a sand-mound of 6 m, a rubble-mound of 4 m and a concrete retaining wall of 6 m were then built in order. The sand drain area was 68 m long and 12 m deep. All of three embankments built on the reclaimed ground were 2 m high. The sea level was set to be 10 m above the top surface of the seabed ground. The bottom of the ground was set to be rigid engineering bedrock in the analysis.

2.2 Determination of soil parameters

The soils in seabed ground and reclaimed ground are regarded as natural deposited soils and exhibit complicated mechanical behaviors that differ from that of remolded soil. For example, naturally deposited clay in a normally consolidated state commonly exhibits softening in undrained shear tests or “rewinding” in a heavily overconsolidated state¹²⁾⁻¹⁴⁾. For this reason, in this study, a series of laboratory tests were carried out on undisturbed clay, and then the behaviors were simulated by using the SYS Cam-clay model.

Firstly, the material constants (elasto-plastic parameters and evolutionary parameters) for each layer are determined by undrained triaxial compression tests and oedometer tests. **Figure 2** shows the simulation results of triaxial test and oedometer test by using the SYS Cam-clay model. In this figure, the bold lines and points are the tests results, and the thin lines the simulation results. In the triaxial test, as shown in **Fig. 2(a)**, each specimen was subjected to an undrained compression under a controlled axial strain rate of 0.0875%/min after 24 hours isotropic consolidation. As shown in **Fig. 2(a)**, the simulation of triaxial test also started from isotropic consolidation and then reproduced shear process. In **Fig. 2(b)**, the specimens were applied on staged load in accordance with the experiment standard of JIS Designation A 1217: 2000. In the simulation of oedometer tests, for each kinds of soil, same material constants (elasto-plastic parameters and evolution parameters) were used as same as those of triaxial tests¹⁴⁾. It can be found that the simulation results can basically describe the mechanical properties of the soils by using the SYS Cam-clay model. Due to the similarity of physical properties, all of the clay layers (AcL, AcU1, AcU2 and AcU3) and dredged soil layer (Bc) are regarded as same material and has same material constants, although the initial values are different. The material

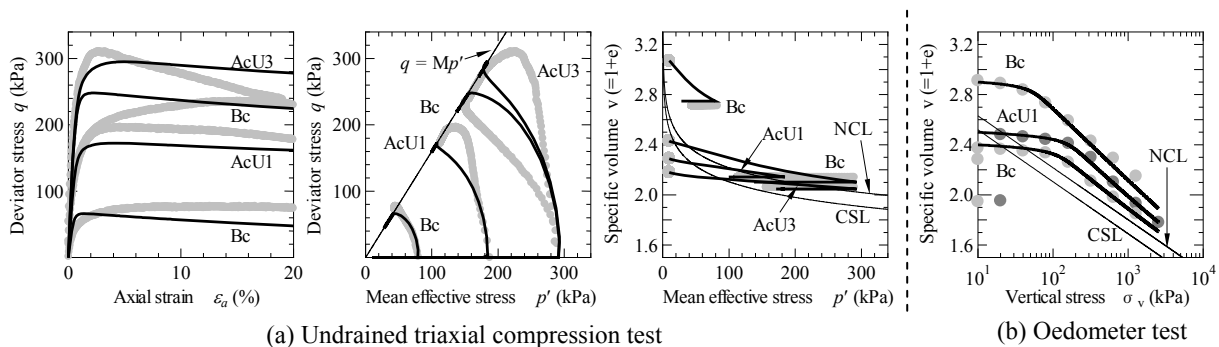


Fig. 2 Simulation results of triaxial test and oedometer test by using the SYS Cam-clay model

constants of sand layer (As) were obtained from the past study¹⁵. The material constants of clay and sand are listed in **Table 1**. According to the relation between specific volume and mean effective stress (in **Fig. 2(a)**) or vertical stress (in **Fig. 2(b)**), all of initial specific volume of the clay lied beyond of the normal consolidation line, which correspond to the so-called “impossible stress state” with high degree of structure. In the SYS Cam-clay model, the evolution parameters are used to describe the loss of overconsolidation, decay of structure and development of induced anisotropy. As shown in **Table 1**, the degradation parameter of overconsolidation m for clay is larger than that of sand, which means that clay is easier to lose overconsolidation. And decay of structure is described by degradation parameters of structure a , b , and c . For sand, it is easier

Table 1 Material constants

Elasto-plastic parameters		Clay	Sand
Compression index $\tilde{\lambda}$		0.18	0.05
Swelling index $\tilde{\kappa}$		0.019	0.0002
Critical state constant M		1.6	1.1
Intercept of NCL at $p' = 98.1 \text{ kPa}$	N	2.22	1.985
Poisson's ratio ν		0.3	0.3
Evolution parameters		Clay	Sand
Degradation parameter of overconsolidation m		3.0	0.12
Degradation parameter of structure a		0.3	5.0
Degradation parameter of structure b		1.1	1.0
Degradation parameter of structure c		1.0	1.0
Ratio of $-D_v^p$ and D_s^p	c_s	0.4	1.0
Rotational hardening index b_r		0.001	3.0
Rotational hardening limit constant m_b		1.0	0.9

D_s^p : Derivative component of plastic sketching tensor

D_v^p : Mean component of plastic sketching tensor

to decay structure compared with clay. Details about the SYS Cam-clay model are in the references⁷⁾⁻⁹⁾.

Secondly, the initial conditions for each layer are determined by simulating unconfined compression tests with the target specific volume and unconfined compression strength from ground survey. Since the process of landfilling was taken into account in this study, the initial condition of the ground was set to be the state before the reclamation work. Because the results of unconfined compression tests of the clay layers sample after reclamation were available, the initial conditions were configured so as to reproduce the unconfined compression strengths. It was done by assuming the initial conditions of the ground and using the SYS Cam-clay model to calculate the following processes

from the initial state to consolidation of the clay layer in the ground by landfilling (one-dimensional consolidation) → sampling (unloading with constant volume) → unconfined compression test.

Based on the results of previous ground surveys, layer Ac was divided into 4 different layers (AcU1, AcU2, AcU3, and AcL). The simulation results of unconfined compression tests are shown in **Fig. 3** and the comparison results with boring data in 2005~2007 are given in **Figs. 4** and **5**. Considering that the measured data in **Figs. 4** and **5** obtained from many different areas in 2005~2007, it indicates that the initial conditions have been determined appropriately and is available for the following calculation. In addition, the initial values of sand layer (As) were obtained from the past study¹⁵. The initial values are shown in **Table 2**. For clay layers, the initial specific volume decrease from upper layer (AcU) to lower layer (AcL). And due to one dimensional consolidation,

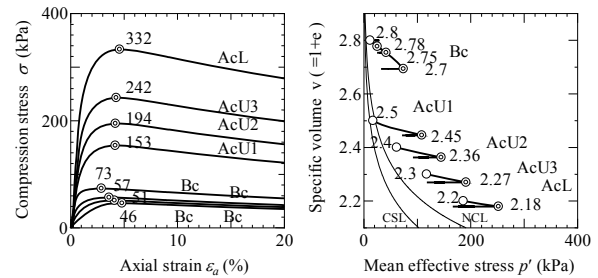


Fig. 3 Simulation results of unconfined compression tests

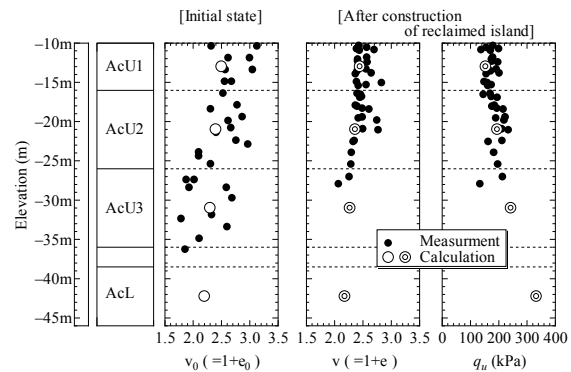


Fig. 4 Simulation and survey results of the soil in seabed ground

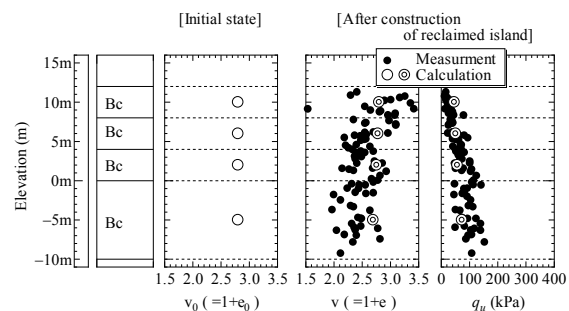


Fig. 5 Simulation and survey results of the soil in reclaimed ground

Table 2 Initial conditions of the soils

Initial value	AcU1	AcU2	AcU3	AcL	Bc	As
Degree of structure $1/R_0^*$	9.0	7.0	5.0	4.0	20.0	2.0
Overconsolidation ratio $1/R_0$	10.8	3.8	2.4	2.2	5.7	12.0
Specific volume $v_0(=1+e_0, e_0: \text{Initial void ratio})$	2.50	2.40	2.30	2.20	2.80	1.84
Stress ratio η_0	0.23	0.23	0.23	0.23	0.0	0.23
Degree of anisotropy ζ_0	0.23	0.23	0.23	0.23	0.0	0.23

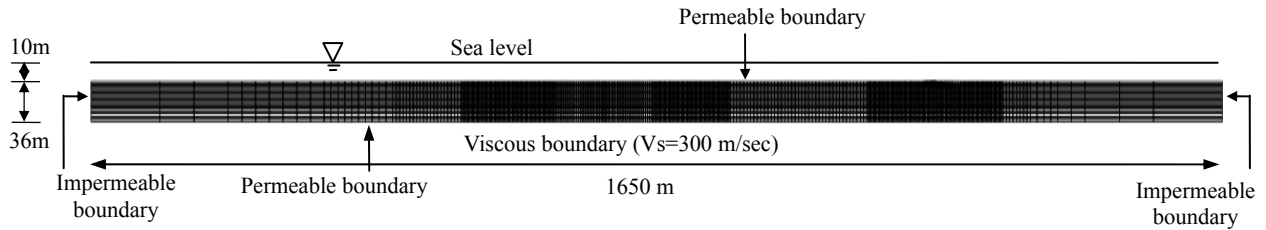


Fig. 6 Finite element mesh for initial seabed ground and boundary conditions

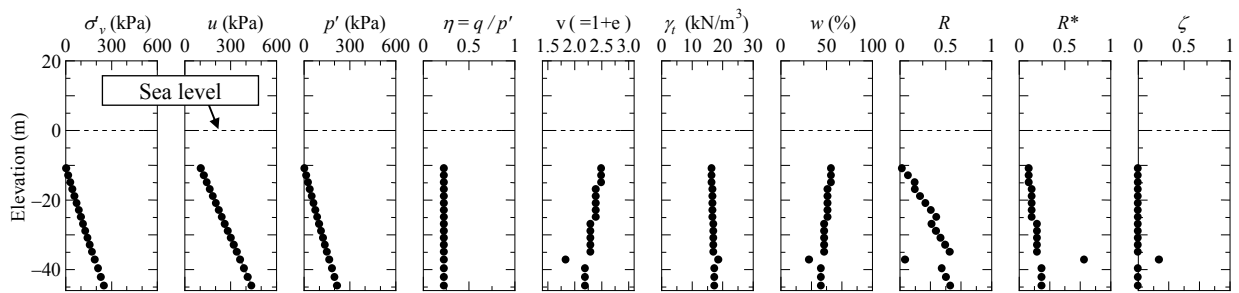


Fig. 7 Initial conditions of the soils in seabed ground

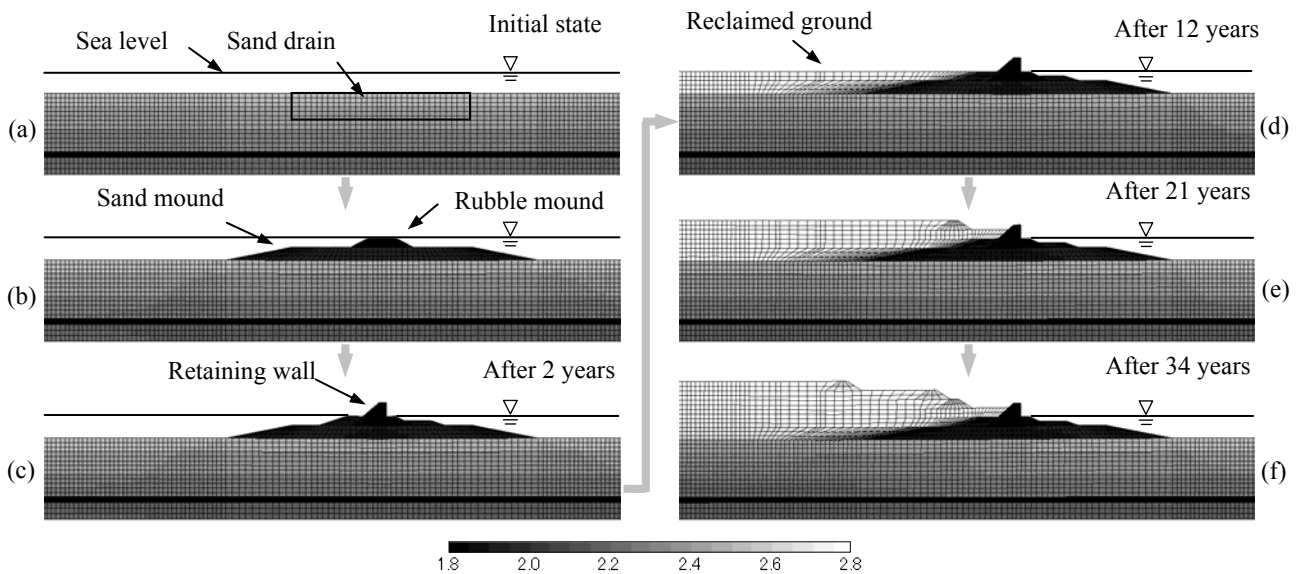


Fig.8 Specific volume distribution of ground near the retaining wall in the construction and reclamation process

the lower layer has smaller initial degree of structure ($1/R_0^*$) and overconsolidation ratio ($1/R_0$). For the

newly reclaimed layer (Bc), the initial degree of structure is higher. Compared with clay, the sand (As) with smaller

$1/R_0^*$ and larger $1/R_0$ is in low structured and heavily overconsolidated state.

3. Calculation of the landfilling process of the reclaimed ground before the earthquake

Figure 6 shows the finite element mesh and boundary conditions of the initial seabed ground before construction and reclamation. The ground is assumed to be horizontally homogenous. And the sea level was set 10 m higher than the top surface of the initial seabed ground, which means that the soil in seabed ground is in fully saturated state. The surface of the seabed ground is considered to be drained condition. And the bottom boundary is also a drained boundary, taking into account of the high permeability of bedrock. The boundary condition which gives simple shear deformation to the finite elements of a side boundary¹⁶⁾ was set to both lateral sides of the ground. The bedrock was made as the engineering base with the shear wave velocity of $V_s=300$ m/s, which is defined as the standard value in the port and harbor construction. The bedrock is dealt with viscous boundary^{17), 18)}.

The initial conditions of the soils in the seabed ground are shown in **Fig. 7**. Based on the initial conditions listed in **Table 2**, it was assumed that the stress ratio η , specific volume v , degree of structure $1/R^*$ and degree of anisotropy ζ of the elements in each layer were uniformly distributed along the depth. The overconsolidation ratio $1/R$ remained constant within each layer, the initial values remain constant.

According to the history of Port of Nagoya¹⁹⁾, the construction and reclamation processes were reproduced and then the current state of the soils in the island were obtained. **Figure 8** shows the change of specific volume during the processes of construction of retaining wall and ground reclamation. Assuming saturated conditions, the reclaimed ground made up of dredged soil was considered to be a two-phase elasto-plastic material, and the simulation was performed by applying the method of finite element addition to the initial ground^{20), 21)}. As

shown in **Fig. 8(a)**, a part of clay in AcU3 layer and AcU2 layer was replaced by sand drain to improve the drainage condition before the construction of upper structure. And then in the following two years, as shown in **Figs. 8 (b) and (c)**, a sand mound, a rubble mound and a concrete retaining wall were built on the replaced area in order. The following works were the embankment construction and ground reclamation. The dredged soil was firstly reclaimed onto the seabed ground. When the height of reclaimed land reached the top surface of embankment, a new embankment was built on the surface of newly reclaimed ground to accommodate more dredged soil. As shown in **Figs. 8 (d)-(f)**, the processes of embankment making and landfilling repeated in the past 34 years and until now the total height of the ground is 20 m from the top surface of the seabed ground. The construction and reclamation processes were carried out exactly as same as actual schedule of the artificial island. By this means, the current state of the soils in the island was obtained and then was set as the referenced initial condition for the following seismic analysis. In the calculation, all of the materials, like clay, sand, sand drain and rubble were regarded as elasto-plastic materials except the concrete retaining wall, which was modeled using linear elastic solid element with Young's modulus $E=23.5$ MPa and Poisson's ratio $\nu=0.2$.

4. Co-seismic and post-seismic analysis

4.1 Two kinds of earthquake ground motions

In the calculation, two kinds of earthquake ground motions, which are short-period ground motion²²⁾ (Type 1) and long-period ground motion²³⁾ (Type 2), are horizontally applied on the nodes of ground base to analyze the seismic responses of the island. The information about the input ground motions is shown in **Fig. 9**, in which the upper figures are the acceleration and the lower figures are the corresponding relation between period and Fourier spectrum. Compared with Type 1 motion, the duration of Type 2 is longer and its maximum acceleration is relative higher. Moreover, the prominent

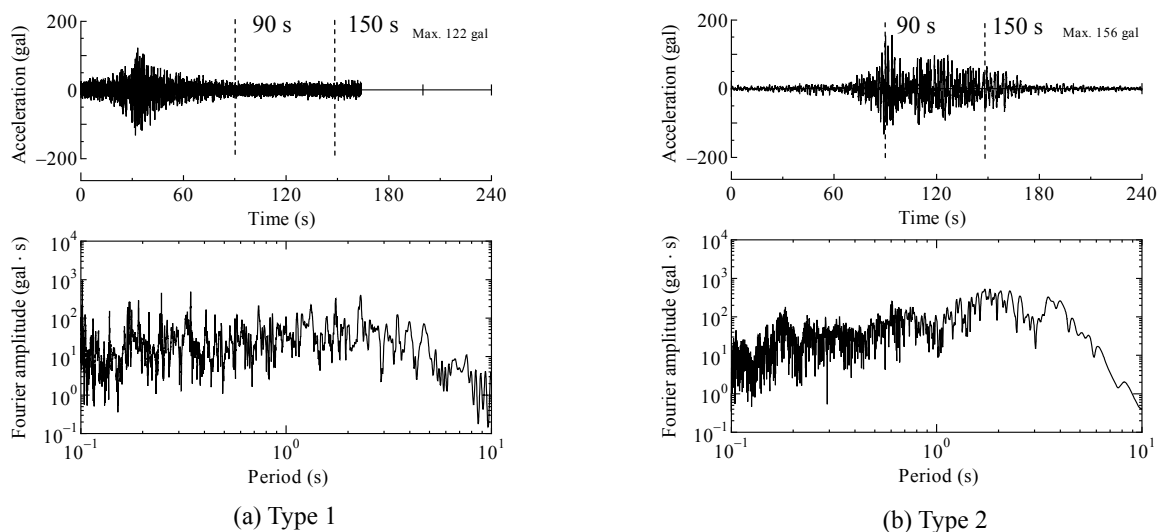


Fig. 9 Two kinds of input ground motions with different spectral characteristics

motions in Type 2 have periods of around 2 seconds, which show different spectral characteristic as Type 1. The seismic response analysis was carried out 5 years after the completion of the ground reclamation.

4.2 Co-seismic and post-seismic analysis results

In this section, special attention was firstly paid to the ground near the retaining wall, where large shear strain was observed. **Figure 10** shows the shear strain distribution of this area with time during and after the earthquake. The state of the artificial island at five years after the final construction and reclamation was set as the initial state in the seismic analysis. As shown in **Fig. 10(a)**, small shear deformation is found at the bottom of reclaimed ground layer due to the development of one dimensional consolidation, which suggests that the soil in same layer were in different condition. It is therefore necessary to reproduce the construction process and obtain the current state distribution of the soils after construction.

The evolution of shear strain with time at 90 seconds, 150 seconds and 16 years after the occurrence of

earthquake is shown in **Figs. 10 (b)-(d)** respectively. In **Fig. 10**, in both Type 1 and Type 2, it shows that large shear deformation occurred in the reclaimed ground (Bc layer) compared with the sea bed ground. The shear deformation areas firstly appeared under the embankment 1 (Emb. 1 for short) and embankment 3 (Emb. 3 for short), and then increased with earthquake shaking and extended to each other. In **Fig. 10(b)**, at 90 seconds after the start of earthquake, larger shear strain occurred under Type 1, of which the mainshock is earlier than Type 2. However, in other stages, larger shear strains were caused by Type 2, because of the longer mainshock duration and larger maximum acceleration of Type 2. In Type 1, the shear strain distribution changed smoothly with depth. By contrast, in Type 2, especially in the Bc layer, a large shear strained areas (from Area D to E in **Fig. 10(d)**) and a slide surface were observed. It suggests that the distribution of shear strain is highly inhomogeneous in Bc layer.

The displacement at two sections (Section A and B in **Fig. 10(a)**) and the mechanical behavior of the soil elements in three areas (Area C, D and E in **Fig. 10(d)**)

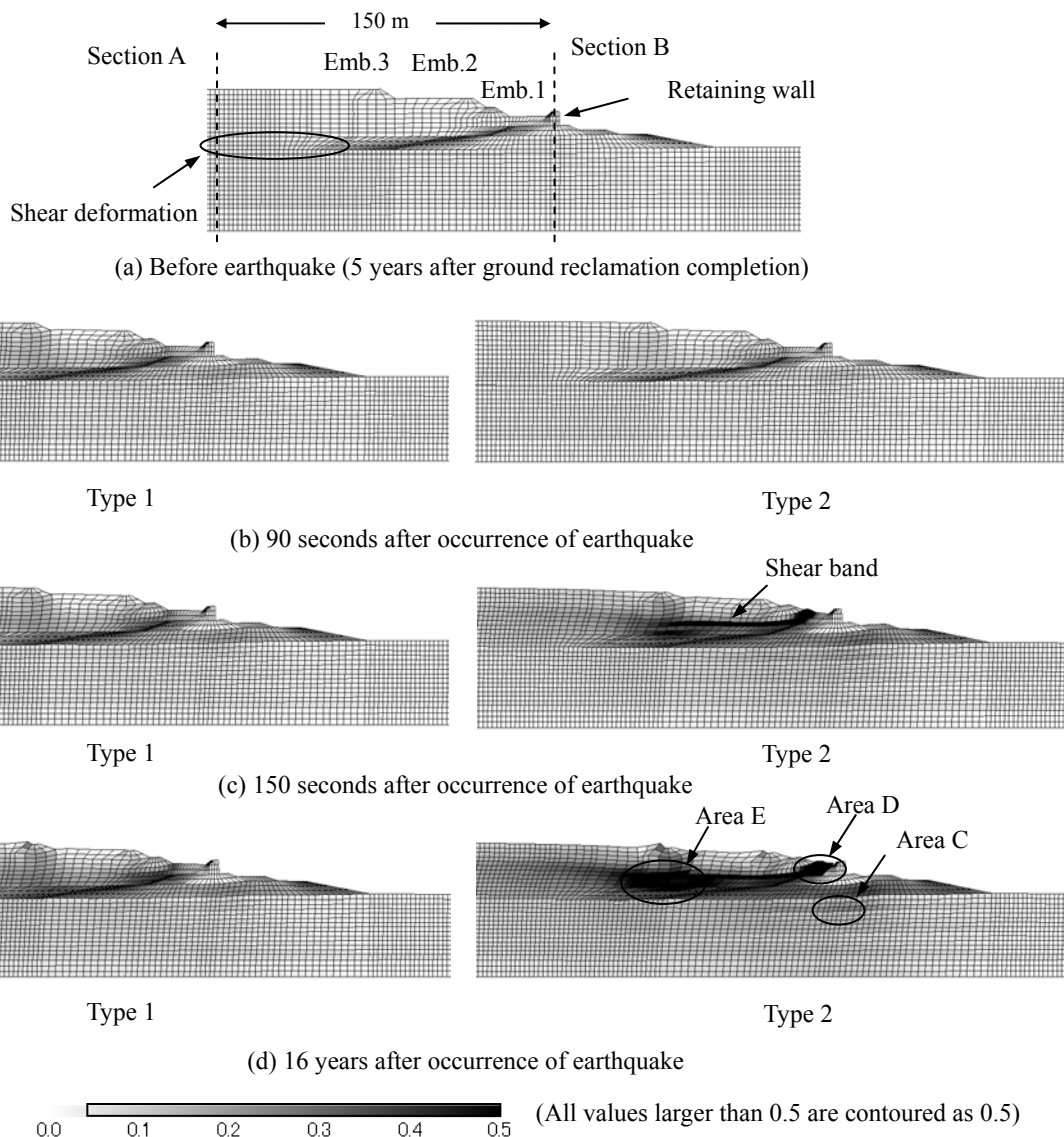


Fig. 10 Distribution of shear strain of the ground near the retaining wall

are illustrated in the following.

(1) Horizontal displacement

The horizontal displacement at two sections (Section A and Section B) is shown in Fig. 11. It can be found that larger horizontal displacements were caused by Type 2. In Fig. 11(a), the ground surface displacement of Type 1 and Type 2 was 1.9 m and 5.1 m at Section A, respectively. While in Fig. 11(b), the displacement of Type 1 and Type 2 was 3.9 m and 7.4 m at Section B, respectively. The displacement at the retaining wall caused by Type 2 is much larger than that of Type 1. In addition, as shown in Fig. 11(a), the increase rate of displacement in reclaimed ground was faster than that in seabed ground. It is because the soil in reclaimed ground is in a relative loose state (specific volume $v: 2.8$) compared with the soil in seabed ground ($v: 2.2\sim 2.5$). It also can be found in Fig. 11(b), though it is not as obvious as that in Fig. 11(a) because of the constraint effect of the retaining wall.

(2) Settlement of the retaining wall

Figure 12 shows the settlement curve of the retaining wall during and after earthquake. The settlement process can be mainly divided into two stages: (1) immediate settlement during the earthquake and (2) large settlement after the earthquake. The first stage is from the beginning to the end of earthquake, in which the settlement during earthquake is 0.49 m (Type 1) and 0.81 m (Type 2). The following settlement after the earthquake is 0.58 m (Type

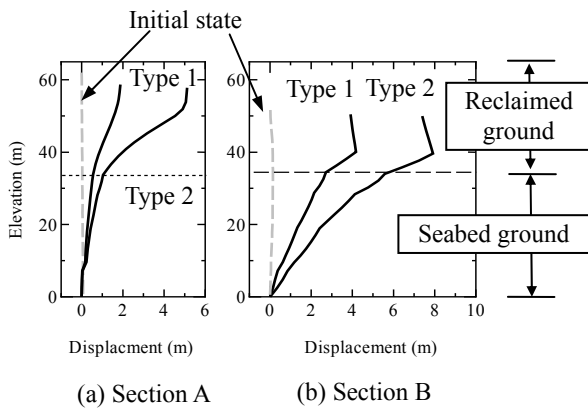


Fig. 11 Horizontal displacement at two sections

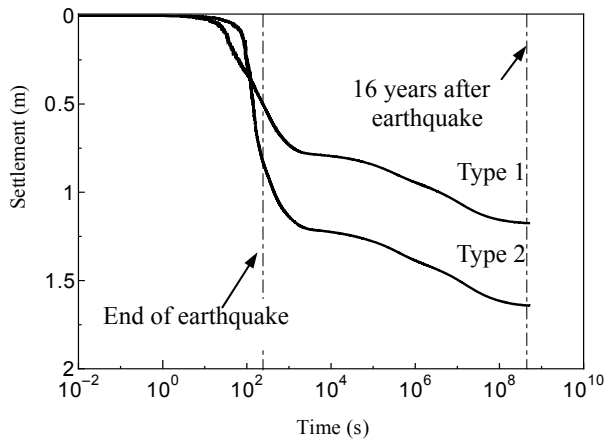


Fig.12 Settlement of the retaining wall during and after earthquake

1) and 0.83 m (Type 2). It can be found that the settlement after earthquake lasts for many years and is even larger than that during earthquake. This kind of “delayed settlement” after earthquake is observed in Mexico earthquake of 1957. The clay layer of 28 m settled about 1.4 m in the following 1500 days after the earthquake²⁴.

5. Interpretation of seismic mechanical behaviors

In this section, the macroscopical responses of the island are explained by the mechanical behaviors of soil elements. The elements of the seabed ground in Area C, which is directly under the retaining wall shown in Fig. 10(d), are chosen to interpret the settlement of the retaining wall. In Fig. 10(d), the shear strain of the reclaimed ground in Areas D and E in Type 2 are much larger than that of Type 1. Thus, the mechanical behaviors of the elements in these three areas are investigated in the following sub-sections.

In the SYS Cam-clay model, the degree of structure and overconsolidation ratio are expressed as $1/R^*$ and $1/R$, respectively. Both R^* and R vary in the range from 0 to 1. The closer R^* to 0 the higher the degree of structure while the soil changes into remodeled state (no structure) when R^* equals to 1. Similarly, the closer R is to 0 the higher overconsolidation ratio of soil; and when R approaches to 1, the soil changes to be normally consolidated state. The details of the SYS Cam-clay model can be found in the references⁷⁻⁹.

5.1 The settlement after the earthquake

In Fig. 12, the simulation result of the settlement curve seems to be similar to the settlement after the earthquake often observed in clay^{21), 25}). The responses of the element in Area C under Type 2 motion are shown in Fig. 13. The response of this element under Type 2 is similar to that

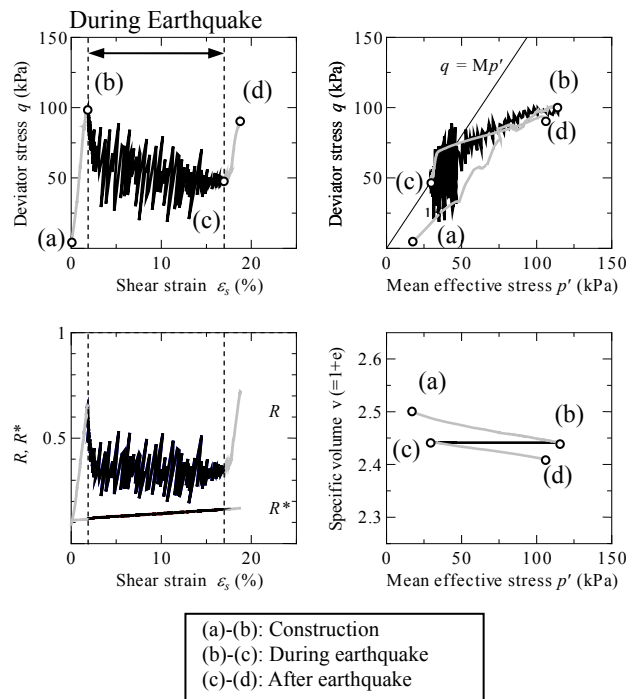
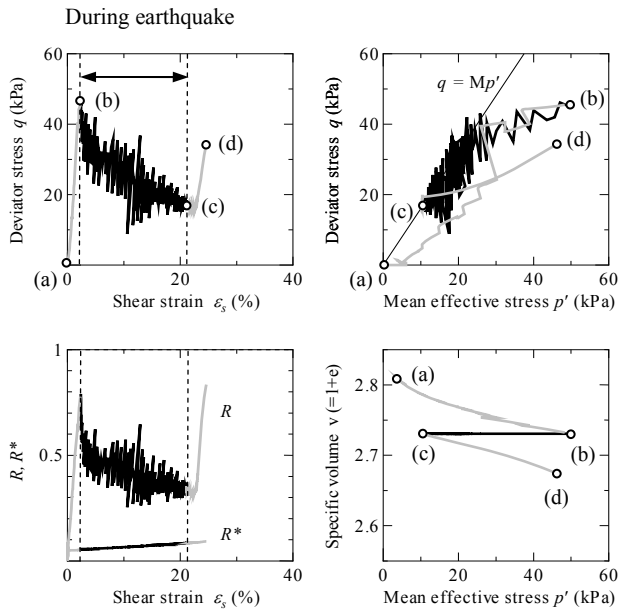
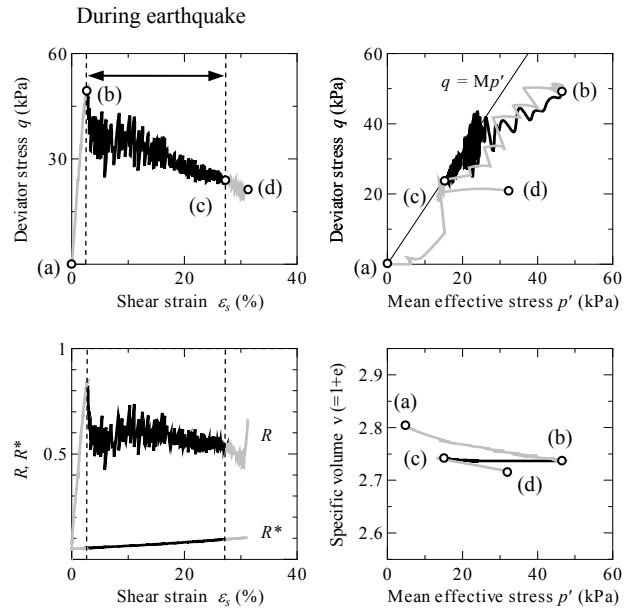


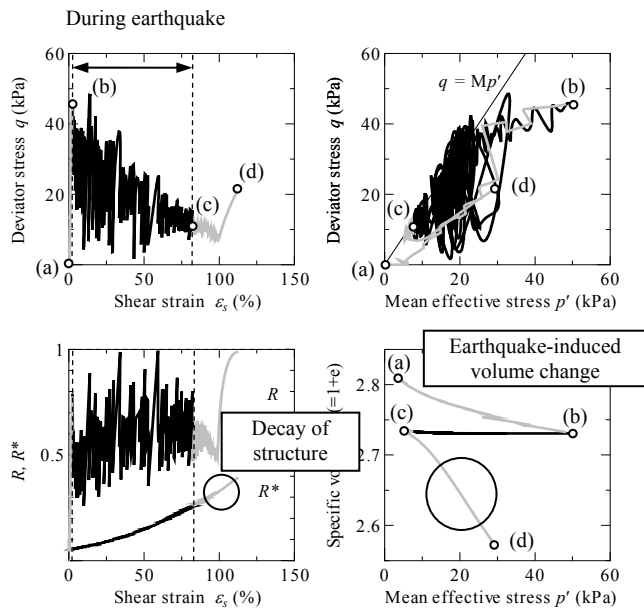
Fig. 13 Responses of the soil directly below the retaining wall (in Area C)



(a) Type 1

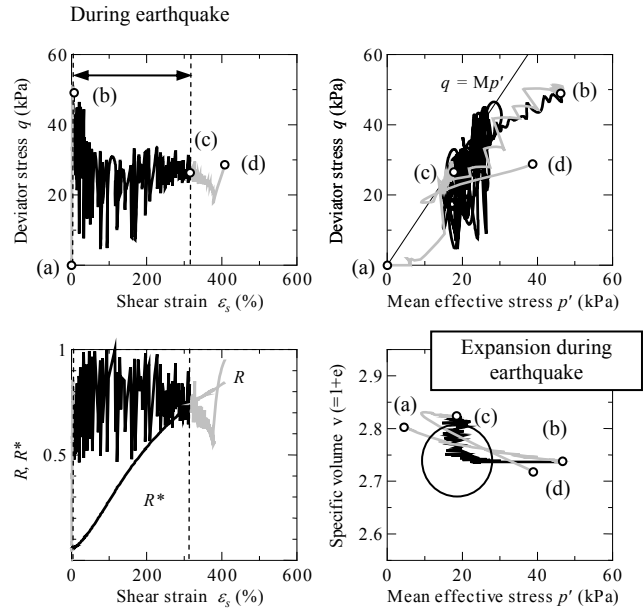


(a) Type 1



(b) Type 2

(a)-(b): Construction
 (b)-(c): During earthquake
 (c)-(d): After earthquake



(b) Type 2

(a)-(b): Construction
 (b)-(c): During earthquake
 (c)-(d): After earthquake

Fig. 14 Responses of high-structured overconsolidated clay during and after earthquake (in Area E)

Fig. 15 Different responses of the soil element during earthquake (in Area D)

under Type 1 except the value of the shear strain. Therefore, the response of the element directly below the retaining wall under the Type 2 motion will be observed to interpret the “delayed settlement” of the retaining wall.

As shown in **Fig. 13**, the behaviors of the soil element in Area C during construction, during earthquake and

after earthquake are indicated by (a)-(b), (b)-(c) and (c)-(d), respectively. It can be found that the shear strain mainly produced during earthquake shaking ((b)→(c)). However, during the earthquake, there was hardly any volume strain in a short time, and consequently, the shear deformation under undrained condition is prominent and the excess pore pressure increases. After earthquake, due

to the low permeability of reclaimed ground, it took long time for the excess pore water pressure to dissipate and the settlement was resulted from consolidation.

5.2 Earthquake-induced settlement

The responses of the elements in Area E in Fig. 10(d) are shown in Fig. 14. The response of the soil in Type 1 seems to be similar to that in Area C and the mechanism of the settlement after the earthquake is the same as that in Area C. However, the response in Type 1 is different from that in Type 2 in the Area E. It is need to consider an additional mechanism about the volume change. That means the volume change due to loss of overconsolidation and decay of structure. The volume change of the highly structured and heavily overconsolidated soil is much different after earthquake motion Type 1 and Type 2.

After earthquake, the soil in Type 2 is in a relative lightly overconsolidated and low structured state compared with the soil in Type 1. Moreover, after earthquake Type 2, as shown in Fig. 14(b), there is obvious to decay of structure in Type 2, while the decay of structure in Type 1 in Fig. 14(a) is very limited. Both element response of soil in Type 1 and Type 2 exhibit loss of overconsolidation (R increased) after the earthquake. However, it is difficult to compare the degree of loss of overconsolidation in Type 1 with that in Type 2. It is clear that the degree of the decay of structure in Type 2 is prominent compared with that in Type 1. Therefore, larger degree of decay of structure in Type 2 cause much larger volume change than Type 1, which can be found in the relation of specific volume and mean effective stress in Fig. 14. It is hard for clay to decay the structure, in other words, the increase of R^* is very limited, even in Type 1 with the shear strain over 20%. However, when the shear strain is large enough as much as that in Type 2, very large volume change can be produced due to decay of structure. And it can be regarded as the reason of earthquake-induced settlement in clay layer.

5.3 Expansion during earthquake

The responses of the soil element in Area D in Fig. 10(d) are shown in Fig. 15. According to the calculated results of specific volume change, as shown in Figs. 13 and 14, the earthquake is generally regarded as an undrained shear process. However, as shown in Fig. 15 (b), the expansion of soil element is observed under the earthquake Type 2. This element located in the large shear strain area between the first soil embankment and the retaining wall, and the shear strain was over 300% during earthquake and achieved 400% after earthquake.

6. Conclusions

In this research, the co-seismic and post-seismic behaviors of an offshore artificial island composed of dredged soil under the condition of two kinds of earthquake motions are investigated by using a soil-water coupled finite element analysis code—*GEOASIA*. The material constants are determined by triaxial test and oedometer test and the initial conditions are determined

by unconfined test respectively. The construction and reclamation process are reproduced to obtain the current state of the ground. Based on the study presented, the following conclusions can be made:

(1) It is possible to determine the initial conditions of the soils in the ground through triaxial test and oedometer test, by computing the process of building up the reclaimed ground with reproducing the unconfined compressive strength and specific volume distribution that had been obtained from ground survey data. It can be found that the state of soil changed with the construction and reclamation process. Small shear deformation is observed at the bottom of the reclaimed ground. It will affect the seismic response of soil and it is thus necessary to consider the construction in calculation.

(2) In the case of earthquake Type 1, the horizontal displacement of the retaining wall is about 3.9m, and in the case of earthquake Type 2, the value is 7.4 m. The horizontal displacement of the reclaimed ground surface 150 m from the retaining wall is 1.9 m and 5.1 m, respectively.

(3) In earthquake Type 1, the settlement of the retaining wall during and after earthquake is 0.49 m and 0.81 m. And in Type 2, the value is 0.58 m and 0.83 m respectively. The “delayed settlement” after earthquake lasts for many years and is even larger than that during earthquake.

(4) In some area with large shear strain ($>75\%$), for the dredged soil with high structure, additional volumetric strain is produced by the decay of structure and therefore earthquake induced settlement is observed, while the volume expansion of soil element during earthquake is observed in the localization of the shear strain ($>300\%$) between the embankment 1 and the retaining wall.

REFERENCES

- 1) Iai, S., Ichii, K., Lui, H. and Morita, T. (1998): Effective stress analyses of port structures, *Soils and Foundations*, Special Issue of Geotechnical Aspects of the January 17 1995 Hyogoken-Nambu Earthquake, 2, 97-114.
- 2) Oka, F., Sugito, M., Yashima and Taguchi, Y. (1997): Three dimensional liquefaction analysis of reclaimed island, *Proc. 7th Int. Offshore and Polar Engineering Conf.*, Honolulu, 1, 665-670.
- 3) Uzuoka, R., Sento, N., Kazama, M., Zhang, F., Yashima, A. and Oka, F. (2007): Three-dimensional numerical simulation of earthquake damage to group-piles in a liquefied ground, *Soil dynamics and earthquake engineering*, 27, 395-413.
- 4) Yang, J., Sato, T. and Li, X.S., (2000): Nonlinear site effects on strong ground motion at a reclaimed island, *Canadian Geotechnical Journal*, 37, 26-39.
- 5) Asaoka A. and Noda T. (2007): All soils all states all round geo-analysis integration, *International Workshop on Constitutive Modeling -Development, Implementation, Evaluation, and Application*, HongKong, China, 11-27.
- 6) Noda, T., Asaoka, A. and Nakano, M. (2008): Soil-water coupled finite deformation analysis based

- no a rate-type equation of motion incorporating the SYS Cam-clay model, *Soils and Foundations*, 48(6), 771-790.
- 7) Asaoka, A., Nakano, M. and Noda, T. (1998): Superloading yield surface concept for the saturated structured soils, *Proc. 4th Euro-pean Conf. on Numerical Methods in Geotechnical Engineering*, Udine, Italy, 233-242.
 - 8) Asaoka, A., Nakano, M. and Noda, T. (2000): Superloading yield surface concept for highly structured soil behavior, *Soils and Foundations*, 40(2), 99-110.
 - 9) Asaoka, A., Noda, T., Yamada, E., Kaneda, K. and Nakano, M. (2002): An elasto-plastic description of two distinct volume change mechanics of soils, *Soils and Foundations*, 42(5), 45-57.
 - 10) Nakai, K., Noda, T. and Asaoka, A. (2009): Numerical simulation of centrifugal model tests on seismic response of embankment-foundation system. *Proc. of 4th International Workshop on New Frontiers in Computational Geomechanics (IWS-Pittsburgh 2008)*, 29-32.
 - 11) Takaine, T., Tashiro, M., Shina, T., Noda, T. and Asaoka, A. (2010): Predictive simulation of deformation and failure of peat-calcareous soil layered ground due to multistage test embankment loading, *Soils and Foundations*, 50(2), 245-260.
 - 12) Asaoka A. (2003): Consolidation of Clay and Compaction of Sand-An elasto-plastic description-, *Proc. 12th Asian Regional Conf. on Soil Mechanics and Geotechnical Engineering*, Singapore, 2, 1157-1195(Keynote lecture).
 - 13) Tatsuoka, F. and Kohata, Y. (1995): Stiffness of hard soils and soft rocks in engineering applications, *Proc. 1st Int. Conf. on Pre-Failure Deformation Characteristics of Geomaterials*, Sapporo, Japan, 2, 947-1063.
 - 14) Nakano, M., Nakai, K., Noda, T. and Asaoka, A. (2005): Simulation of shear and one-dimensional compression behavior of naturally deposited clays by Super/subloading Yield Surface Cam-clay model, *Soils and Foundations*, 45(1), 141-151.
 - 15) Ito, Y. (2009): Numerical analysis on seismic behavior of Port Island modeled in consideration of a reclaimed history, Master Dissertation, Department of Civil Engineering, Nagoya University, Nagoya, Japan.
 - 16) Yoshimi, Y. and Fukutake, K. (2005): Physics and evaluation technology of soil liquefaction including mitigation method, Gihodo-Shuppan (in Japanese).
 - 17) Lysmer, J. and Kuhlemeyer, R. L. (1969): Finite dynamic model for infinite media, *ASCE*, 95(EM4), 859-877.
 - 18) Joyner, W. B. and Chen, A. T. F. (1975): Calculation of nonlinear ground response in earthquake, *Bulletin of the Seismological Society of America*, 65(5), 1315-1336.
 - 19) Nagoya Port Authority (1990): History of Nagoya Port, Construction Section (in Japanese).
 - 20) Takeuchi, H., Takaine, T. and Noda, T. (2006): Effect of change in geometry on soil-water coupled deformation of clay soil, *Journal of Applied Mechanics*, JSCE, 9, 539-550 (in Japanese).
 - 21) Noda, T., Takeuchi, H., Nakai, K. and Asaoka, A. (2009): Co-seismic and post-seismic behavior of an alternately layered sand-clay ground and embankment system accompanied by soil disturbance, *Soils and Foundations*, 49(5), 739-756.
 - 22) National Institute for land and infrastructure management, Ministry of land, infrastructure, transportation and tourism: <http://www.ysk.nilim.go.jp/kakubu/kouwan/sisetu/sisetu.html>
 - 23) Central Disaster Prevention Council Cabinet Office, Government of Japan. (2004): Published data of Tohankai-Nankai earthquake.
 - 24) Zeevaert, L. (1984): Foundation engineering for difficult subsoil conditions (2nd edition), Van Nostrand Co. Ltd.
 - 25) Noda, T., Asaoka, A., Nakano, M., Yamada, E. and Tashiro, M. (2005): Progressive consolidation settlement of naturally deposited clayey soil under embankment loading, *Soils and Foundations*, 45(5), 39-51.

(Received: March 9, 2010)